Deep Learning Aided Resource Allocation in Hybrid NOMA-Enabled Overloaded Systems

Simon Chege* and Tom Walingo
Discipline of Electrical, Electronics and Computer Engineering, University of Kwa Zulu Natal, Durban, South Africa
Email: schegemathinji@gmail.com (S.C.), walingo@ukzn.ac.za (T.W.)

Manuscript received July 3 2024; revised September 4, 2024; accepted September 30, 2024
*Corresponding author

***Abstract*—Beyond 5G (B5G) networks will deploy hybrid multi-radio access technologies for improved Spectrum Efficiency (SE) and Energy Efficiency (EE). For further capacity enhancement, code and power domain multiplexing are applied on hybrid Power Domain Sparse Code Non-orthogonal Multiple Access (PD-SCMA) schemes. In order to realize optimal performance, robust Resource Allocation (RA) policies are required with the best candidate for the complex overloaded B5G systems based on Artificial Intelligence (AI) techniques. This work develops a deep neural network (DNN) aided resource allocation scheme for an uplink PD-SCMA network with Near-User (NU) and Far-User (FU) groups, multiplexed in the power and code domain. The RA problem is formulated as a non-convex joint optimization problem then decomposed into three sub-problems namely Codebook Assignment (CA), User Clustering (UC) and power allocation (PA). For the three sub-problems, a three-stage generic fully connected DNN is trained to approximate the PA, CA and UC resource allocation solution by the proposed modified Primal-Dual Interior Point Method (mPD-IPM). The proposed mPD-IPM generates the near-optimal RA solutions that form the DNN input labels. The DNN-mPD-IPM not only greatly enhances the computational efficiency but also achieves improved convergence rates and guarantees both the ergodic and non-ergodic sum rates of the system compared to generic algorithms. Simulation results show that the DNN aided resource allocation closely learns the system capacity and computational performance of the proposed mPD-IPM and further outperforms generic RA algorithms. Compared to cross-layer codebooks, mPD-IPM and DNN-mPD-IPM achieves approximately 19% higher capacity. The proposed DNN-mPD-IPM that learns to approximate the proposed mPD-IPM has an execution time that is approximately 70% lower than mPD-IPM.**

***Index Terms*—Deep neural networks, Power Domain Sparse Code Non-Orthogonal Multiple Access (PD-SCMA), primal-dual interior point method, resource allocation, system capacity**

I. Introduction

The need for advanced multi-radio technologies for increased bandwidth, Spectrum Efficiency (SE) and Energy Efficiency (EE) for current and Beyond 5G (B5G) thirsty network applications need not be reemphasized: Non-Orthogonal Multiple Access (NOMA) schemes have been developed for spectral efficiency enhancement in divergent application scenarios compared to the conventional Orthogonal Multiple Access (OMA) scheme [1], Hybrid NOMA schemes that employ multiplexing to support highly overloaded multi-user systems have also been developed [2–6]. Multiple users are multiplexed on a single resource element in the code domain such as in Sparse Code Multiple Access (SCMA) [7], or power domain for Power Domain Non-Orthogonal Multiple Access (PD-NOMA) [8] and in both domains for the hybrid NOMA. As an example, in the hybrid Power Domain Sparse Code Non-Orthogonal Multiple Access (PD-SCMA), Near-User equipments (NUs) and far-user equipments (FUs) are co-multiplexed using PD-NOMA into a codebook, while allocating distinct power levels and hence applying Successive Interference Cancellation (SIC) for their detection at the receiver. Furthermore, different codes are exclusively assigned to the NU-FU clusters, hence employing any of the various versions of the Message Passing Algorithm (MPA) based detectors [9].

The PD-SCMA multiplexing performance is a function of resource management at the transmitter, interference management in the channel and Multi-User Detection (MUD) at the receiver. The development of optimal resource allocation (RA) schemes including Codebook Assignment (CA), User Clustering (UC) and Power Allocation (PA) in PD-SCMA is needed for optimal performance and is a challenging task. In [3], NUs cluster and FUs cluster were simultaneously supported in PD-NOMA while data for NUs was transmitted by SCMA scheme. The joint access scheme significantly improves the system throughput compared to the conventional OMA. For purposes of improving spectral sharing, the work in [4] developed a numerical analysis for the proposed PSMA that allows overloading in both power and code domains. Additionally, authors in [5] explored joint power-domain and SCMA-based NOMA system for downlink in B5G, in order to increase the number of supported User Equipments (UEs). The work in [6] proposed biological based RA schemes, namely, the Ant Colony Optimization (ACO), Particle Swarm Optimization (PSO) and a hybrid Adaptive Particle Swarm Optimization (APASO) algorithms for an uplink PD-SCMA aimed at enhancing the system sum-rate and energy efficiency. For these schemes, a joint MUD based on SIC and MPA variants are employed to decode the transmitted signals. Furthermore, the PD-SCMA hybrid NOMA closed-form solutions for codebook, pairing and power multiplexing capacity

doi: 10.18178/ijeetc.14.1.1-12

bounds were derived in [9], with RA challenges highlighted. These challenges necessitate different modern methods for RA in B5G networks.

The evolution of Artificial Intelligence (AI) has occasioned the development of machine learning algorithms. As a subset of machine learning, Deep Learning (DL) has found applications in advancing and realization of the full potential of B5G networks due to its superior handling, processing and analysis of huge data with diverse degrees of complex networks, compared to conventional machine learning techniques in [10]. Recently, DL architectures find applications in diverse domains of wireless B5G networks producing faster, easily configurable, more consistent and reliable results. DL algorithms are implemented using Neural Networks (NN) consisting of input, hidden and output layers as outlined in [11]. In NOMA systems, DL algorithms have recently been applied in enhancing SE and EE, massive connectivity and latency reduction [12–14]. Basically, in NOMA, two types of learning can be adopted, namely, offline and online Deep Neural Network (DNN) learning. In offline training, Channel State Information (CSI) of diverse environments fetched from input sequences and simulations are substantially trained. Conversely, in online training, the input signal is trained with real-time CSI helped by the pilot signals data. The authors in [12] applied a DL based Long Short Term Memory (LSTM) network in NOMA environment with randomly deployed users but served by same Base Station (BS). Here, the LSTM is trained offline by simulated data under disparate channel conditions, then deployed online. A DNN algorithm was employed in [13] to predict the power allocation for optimized Energy Efficiency (EE) in an imperfect SIC. A DNN that incorporates random user activation and symbol spreading was deployed to enhance the reliability of grant-free NOMA in [14] for low-latency Internet of Things (IoT) applications. The DNN learns by utilizing a multi-loss function where the penalty is based on user activation probability. In a bid to optimize RA schemes, thereby minimizing the computational complexity and time, B5G NOMA schemes have embraced DL based algorithms. The authors in [15] investigated an energy efficient Deep Reinforcement Learning (DRL)-assisted RA for Radio Access Network (RAN) slicing flexibility. By making full use of channel information, the work in [16] explored a RA scheme using DL architecture to follow the status of channel and help the flexible and precise allocation scheme. Compared to traditional resource optimization schemes, the proposed model exhibits significant performance improvement and reduced computational time. A supervised DL model to solve the sub-band and power allocation problem in a multi-cell network was proposed in [17]. In the work [18], RA for uni-cast and multi-cast services of multimedia TV broadcasting was proposed; a LSTM based DL model constructed the dynamic space-time traffic model of the multi-cast service thereby providing a basis for further network RA; and then a DRL framework was deployed for the RA optimization. In order to accommodate diverse Quality of Service (QoS) requirements in B5G networks, authors in [19] proposed a cascaded NN structure where the first NN estimated the optimal bandwidth allocation while the second NN estimated the power allocation for QoS satisfaction. The performance of the cascaded NN outdoes that of the fully connected NN structure in terms of QoS guarantee. However, these works do not address the hybrid NOMA schemes.

In comparison to genetic RA algorithms, DL based RA algorithms have exhibited great potential in improving system throughput in SCMA. Authors in [20] explored the generation of codebooks, then deploys multiple basic DNN units between signal streams and resources such that these DNN units can learn the appropriate mapping. A RA (codebook allocation and power distribution) algorithm based on LSTM and dueling Deep Q Network (DQN) was proposed in [21] for SCMA based Multi-Access Edge Computing (MEC) networks aimed at maximizing the computational time in a resource-constrained IoT devices. In an attempt to avoid Inter-Cell Interference (ICI) for SCMA users, the work in [22] investigated a strategy of radio RA based on LSTM. The input to the LSTM network constitutes the interference power received at individual resource blocks predicted before signal transmission. The resource blocks with less predicted interference are then selected for signal transmission thereby exhibiting great potential in ICI avoidance. Authors in [23] proposed an auto-encoder based on DNN that combines encoding and decoding together for near optimal codebook generation and signal bits reconstruction for a dense SCMA.

To further realize benefits that come with NOMA namely, spectrum sharing efficiency, overloading and energy efficiency, several works have proposed and investigated the performance of hybrid NOMA schemes in [2–6, 9]. In these schemes, generic algorithms such as SCOA, OMSP and QAPA in [2], DPR-RA in [9] and biological RA schemes in [6], and conventional MUDs such as SIC, MPA, EPA and their combinations are proposed for RA and detection respectively. Although there has been significant effort to improve allocation strategies of radio resources at transmission as well as signal detection and reconstruction at reception, generic algorithms still exhibit sub-optimality. Besides, with increased resource overloading, generic algorithms saturate thereby limiting the multiplexing potential of a hybrid NOMA scheme. In addition, the generic RA and MUDs based architectures exhibit increased computational complexity and take longer computational time as the number of user equipment in the system bulge. Given the potential associated with DL in radio resource management, in both PD-NOMA and SCMA, this work considers the deployment of DNN based resource allocation model for a hybrid NOMA scheme.

Previously, significant works have been done in optimizing RA and detection via DL in SCMA and PD-NOMA separately and only a few works have focused DL deployment for hybrid NOMA. In [24], an uplink hybrid NOMA scheme (HMAS) that jointly adopts Orthogonal Frequency Division Multiple Access (OFDMA) and SCMA to support NUs and FUs respectively was developed. Two DNN based detectors which are trained offline via simulated data and applied online for real-time detection are proposed for each user group. The proposed

detector significantly outperforms the conventional joint MPA-SIC detector. An iterative cross-physical-and application-layer codebook allocation for uplink PD-NOMA SCMA video communications was proposed in [25]. Firstly, the codebooks are assigned generically using the physical layer Channel State Information (CSI) then exchanged within users intentionally to minimize the MSE therewith, increasing the Peak to Signal Noise Ratio (PSNR). To reduce the computational complexity and further optimize the CA, a DNN approach is proposed, which significantly improves the video PSNR, reduces the execution time albeit a slight performance degradation. The RA in hybrid NOMA is a multi-dimensional problem. However, authors in [25] only considered the codebook allocation of the hybrid PD-SCMA.

This work develops and investigates two resource allocation schemes namely, modified Primal-Dual Interior Point Method (mPD-IPM) and DNN aided mPD-IPM (DNN-mPD-IPM) for an uplink hybrid PD-SCMA network. The developed RA schemes feature UEs channel gains, UE distance to BS, NU and FU cluster power level distinctiveness and interference threshold. The RA problem is formulated as a Mixed-Integer Non-Linear Programming (MINLP) RA problem. The MINLP optimization problem is decomposed into three sub-problems namely; PA, CA and UC. Firstly, a three-stage mPD-IPM RA is proposed to obtain the optimal PA, CA and UC solutions that are then regarded as the data set label input for the DNN aided RA algorithm. Secondly, an alternate three-stage fully connected DNN-mPD-IPM RA is then trained to approximate the label input, which not only enhances the computational efficiency and convergence rate but also the system capacity. Different from [25] which only considered CA, we explore the joint RA of CA, FUs and NUs clustering and PA. The DNN-mPD-IPM provides a unified framework for optimizing the PD-SCMA RA scheme. Developed results demonstrate that the proposed DNN-mPD-IPM optimizes the mPD-IPM RA scheme and significantly outperforms the benchmark generic RA schemes in terms of improving system performance.

A. Organization

The rest of the paper is organized as follows: the system model and problem formulation are presented in Sections II and III respectively. Section IV and Section V details the proposed mPD-IPM and DNN based RA schemes respectively while Section VI presents the convergence and complexity analysis. In Section VII, simulation results and discussions are presented. Finally, Section VIII concludes the paper.

B. Notation

We denote by x, $\mathbf{x}$, $\mathbf{X}$, and $\mathcal{X}$ a scalar, vector, matrix and set respectively. A set of M-ary numbers is denoted by M. What's more, $\mathbf{x}^T$ and diag($\mathbf{x}$) represent the transpose and diagonal matrix respectively. Besides, diag($\mathbf{x}$) is a vector of the diagonal elements of matrix $\mathbf{X}$. The summary list of all notations and variables is given in Table I.

TABLE I: NOTATION AND VARIABLES

Notation	Meaning
C	Codebooks
J	Codebook size
U	NUs in the BS
N	Resource elements (REs)
$h_{u,c}^{\mathrm{NU}}, h_{k,c}^{\mathrm{FU}}$	Channel fading gains
R	Achievable total system sum rate
$\varepsilon_{u,c}^{\mathrm{NU}}, \varepsilon_{k,c}^{\mathrm{FU}}$	Channel estimation errors
$q_{u,c}^{\mathrm{NU}}, q_{k,c}^{\mathrm{FU}}$	Codebook assignment policies
$A_{k,u}^{c}$	User clustering policy
$P_{u,c}^{\mathrm{NU}}, P_{k,c}^{\mathrm{FU}}$	Power allocation policy
$y_{k,c}^{\mathrm{FU}}$	FU Received signal at BS
K	FUs in a BS
$\mathcal{U}_{\mathrm{CB}}$	Set of NUs paired on codebook C
$\mathcal{I}_{u\to k}^{c,\mathrm{th}}$	Pairing Interference
d_f	No. of UEs in a RE
D	Multiplexing codebook bound
d_v	No. of REs in a codebook
$r_{u,c}^{\mathrm{NU}}, r_{k,c}^{\mathrm{FU}}$	Achievable user sum rate
$x_{u,c}^{\mathrm{NU}}, x_{k,c}^{\mathrm{FU}}$	Transmitted signals

II. SYSTEM MODEL

This article proposes a deep learning aided resource allocation protocols for an uplink hybrid NOMA system to enhance efficient spectrum sharing in overloaded systems such as heterogeneous networks and IoE applications. The utilized system network model is expounded in the following subsections.

A. Uplink PD-NOMA System

The uplink PD-NOMA transceiver model supports K UEs, allocated distinct power levels, transmitting using the same spectrum resources to a common BS. The BS receives the superposed signal message of K UEs denoted by y and deploys SIC to detect each signal.

$$y = \sum_{i=1}^{K} h_i \sqrt{p_i}\, x_i + z \tag{1}$$

where p_i and x_i are the transmit power and signal transmitted by the ith UE, respectively. h_i denotes the channel gain of the ith UE. Furthermore, z associated with the power density N_0 represents the AWGN plus the inter-cell interference (ICI) at the BS.

The PD-NOMA receiver considers that $p_1|h_1|^2 \geq p_2|h_2|^2 \geq \cdots \geq p_K|h_K|^2$, accordingly the optimal decoding order for SIC is $x_1, x_2, \cdots, x_K$. With SIC, the strongest UE signal x_i is decoded first while observing interference from the other UEs [26]. Denoting by Γ the minimum power difference required to distinguish between the signal to be decoded and the remaining non-decoded message signals, the necessary power constraints for efficient SIC in an ith UE uplink NOMA cluster can be expressed as

$$p_i|h_i|^2 - \sum_{j=i+1}^{K} p_j|h_j|^2 \geq \Gamma \tag{2}$$

The major drawback with SIC in B5G networks with multiple selective channels is the ICI due to cumulative decoding errors which increases the decoding complexity at the receiver side therefore limiting the cluster superposing bounds [27].

B. Uplink SCMA System

The uplink SCMA transceiver model supports K UEs transmitting using N Resource Elements (REs). Each UE assigned to a single codebook, utilizes $d_v < N$ REs while each RE can be accessed by $d_f < K$ UEs. The coder operates K symbols $s = [s_1, s_2, \cdots, s_K] \in \mathbb{M}^{1\times K}$ in a cycle, where every $\log_2 M$-bit symbol for the kth UE maps to one of the length $-M$ column vectors with $d_v, (d_v \leq N)$ used REs of sparse codeword matrix $C_k \in \mathbb{C}^{N\times M}$, resulting into complex codeword $x_k \in \mathbb{C}^{N\times 1}, k \in \{1, 2, \cdots, K\}$. The combined codewords from all the K layers form the transmit vector, $\mathbf{x} \in \mathbb{C}^{N\times 1}$, transmitted over N REs. The notation d_v, d_f and $\lambda = K/N$ refers to the codebook sparsity degree, maximum degree of user superposition on a given RE and the overloading factor respectively [7].

The N-dimensional uplink received vector is then given by

$$\mathbf{y} = \sum_{k=1}^{K} \mathbf{H}_k \mathbf{x}_k + \mathbf{z} \tag{3}$$

where $\mathbf{y} = (y_1, y_2, \cdots, y_N)^T$, $\mathbf{x}_k = (x_{k,1}, x_{k,2}, \cdots, x_{k,N})$, $\mathbf{H}_k = \text{diag}(\mathbf{h}_k)$ and $\mathbf{h}_k = (h_{k,1}, \cdots, h_{k,N})$ is the $K\times 1$ channel gain vector of UE k. The $K\times 1$ vector $\mathbf{z}$ corresponds to the AWGN with variance N_0.

The dominant near-optimal SCMA receiver decoding strategies is the MPA and its variants namely; Log-MPA and MaxLog-MPA [2, 9]. The expectation propagation algorithm (EPA) [28, 29], sphere decoding [30] and polar-coded SCMA [31]. Recently, the proposed DL based detection demonstrates significant potential improvement in detection BER performance, reduced complexity and optimized computational time [7].

C. Uplink Hybrid PD-SCMA System

The uplink PD-SCMA transceiver model supports a sets of $\mathcal{U}$ NUs and $\mathcal{K}$ FUs. Similar to the conventional SCMA, a PDSCMA transmitter operates L=K layers (of set $\mathcal{L}$) and N orthogonal resource elements (REs), where $N << L$. Each layer utilizes $d_v, (d_v < N)$ REs, thus, each layer spreads its data over d_v REs. A layer is constructed by drawing select codewords from each UE of FU set $\mathcal{K}, |\mathcal{K}| = K$ and clustered NUset $\mathcal{U}_{CB}, (|\mathcal{U}_{CB}| = U, \mathcal{U}_{CB} \in \mathcal{U})$. This implies that a layer constitutes $D(U+1)$ users symbols. Fig. 1 illustrates the PD-SCMA block diagram with L layers, N=4 REs, $d_v = 2$ in the code-domain and D multiplexed users in the power-domain.

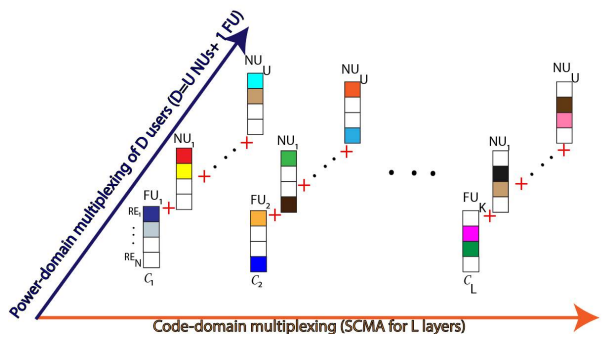

Fig. 1. PD-SCMA block with $D = U + 1, U \in U_{CB}$ superimposed NUs, L layers/codebooks and $N = 4$ REs.

Under the constraint that no two layers should be assigned all the same RUs for an affordable complexity order, a system is fully loaded if $\lambda = D \times \binom{L}{d_v}$, where λ denotes the overloading factor.

At the PD-SCMA transmitter, every $\log_2 M$-bit symbols are encoded to a length -N sparse vector resulting into complex codewords $x_{k,c}^{\text{FU}} = [x^{\text{FU}_{k,1}}, \cdots, x^{\text{FU}_{k,N}}]^T$ and $x_{u,c}^{\text{NU}} = [x^{\text{NU}_{u,1}}, \cdots, x^{\text{NU}_{u,N}}]^T$ for FUs and NUs respectively. The vectors $x_{k,c}^{\text{FU}}$ and $x_{u,c}^{\text{NU}}$ belongs to a finite set of $\mathcal{M}, |\mathcal{M}| = M$ codewords of codebook $\mathcal{C}$. A codebook can be utilized by a single user, (case of the conventional SCMA) or several users, (case as with PD-SCMA) by pairing users with distinct power levels.

Consider the policies applied as defined below:

- The PA policy $\mathbf{p} = \{P_{K,C}^{\text{FU}}, P_{U,C}^{\text{NU}}\}$ is such that the transmitter allocates $P_{K,C}^{\text{FU}} = \left[P_{k,c}^{\text{FU}}\right]_{K\times C}$ power to the kth FU on codebook c and $P_{U,C}^{\text{NU}} = \left[P_{u,c}^{\text{NU}}\right]_{U\times C}$ to the uth NU utilizing the same codebook c. Note that $P_{u,c}^{\text{NU}} \gg P_{k,c}^{\text{FU}}$.
- The CA policy $\mathbf{q} = \{Q_{K,C}^{\text{FU}}\}$ where $Q_{K,C}^{\text{FU}} = \left[q_{k,c}^{\text{FU}}\right]_{K\times C}$ denote FU transmitter CA matrix. Also, $\left[q_{k,c}^{\text{FU}}\right] = 1$ implies that codebook c is assigned to the kth FU.
- The UC policy $\mathbf{a} = \left[A_{k,u}^{c}\right]_{K\times U}$, where $A_{k,u}^{c} = 1$ denotes that the kth FU is paired with the uth NU on codebook c, while $A_{k,u}^{c} = 0$, denotes otherwise.

Let $\mathbf{H} = \{H_{U,C}^{\text{NU}}, H_{K,C}^{\text{FU}}\}$, where $H_{U,C}^{\text{NU}} = \left[h_{u,c}^{\text{NU}}\right]_{U\times C}$ and $H_{K,C}^{\text{FU}} = \left[h_{k,c}^{\text{FU}}\right]_{K\times C}$ denote channel-fading gains of the uth NU and kth FU on codebook c. The statistical channel coefficients are modelled as:

$$h_{u,c}^{\text{NU}} = \hat{h}_{u,c}^{\text{NU}} + \varepsilon_{u,c}^{\text{NU}} \tag{4}$$

$$h_{k,c}^{\text{FU}} = \hat{h}_{k,c}^{\text{FU}} + \varepsilon_{k,c}^{\text{FU}} \tag{5}$$

where $\hat{h}_{u,c}^{\text{NU}} \sim \mathcal{CN}(0, \hat{\sigma}_{u,c}^2)$ and $\hat{h}_{k,c}^{\text{FU}} \sim \mathcal{CN}(0, \hat{\sigma}_{k,c}^2)$ are the estimated channel gains with variances $\hat{\sigma}_{u,c}^2$ and $\hat{\sigma}_{k,c}^2$ respectively. $\varepsilon_{u,c}^{\text{NU}} \sim \mathcal{CN}(0, \sigma_\varepsilon^2)$ and $\varepsilon_{k,c}^{\text{FU}} \sim \mathcal{CN}(0, \sigma_\varepsilon^2)$ denote the channel estimation errors with variance σ_ε^2. It is assumed that estimated channel gains and errors are uncorrelated stationary and ergodic random processes.

Considering that each codebook is exclusively assigned to a single FU at each BS but re-used by NUs, the received signal $y_{k,c}^{\text{FU}}$ is given by:

$$y_{k,c}^{\text{FU}} = q_{k,c}^{\text{FU}} h_{k,c}^{FU} \sqrt{P_{k,c}^{\text{FU}}} x_{k,c}^{\text{FU}} + \sum_{u\in\mathcal{U}_c} A_{k,u}^{c} h_{u,c}^{\text{NU}} \sqrt{P_{u,c}^{\text{NU}}} x_{u,c}^{\text{NU}} + z_{k,c} \tag{6}$$

where $x_{k,c}^{\text{FU}}$ and $x_{u,c}^{\text{NU}}$ are the transmitted signals of the FU and NU on codebook c, respectively, $\mathcal{U}_c$ denotes the set of NUs paired with FU k on codebook c and $z_{k,c} \sim \mathcal{CN}(0, \sigma_{k,c}^2)$ is the additive white Gaussian noise power (AWGN). The achievable throughput at the BS, $r_{u,c}^{\text{NU}}$ and $r_{k,c}^{\text{FU}}$ are respectively given by:

$$r_{u,c}^{\text{NU}} = B_{\text{RE}} \log_2\left(1 + \gamma_{u,c}^{\text{NU}}\right) \tag{7}$$

$$r_{k,c}^{\text{FU}} = B_{\text{RE}} \log_2\left(1 + \gamma_{k,c}^{\text{FU}}\right) \tag{8}$$

where $\gamma_{u,c}^{\mathrm{NU}}$ and $\gamma_{k,c}^{\mathrm{FU}}$ are the signal to interference and noise ratio (SINR) of the *u*th NU and *k*th FU on codebook *c* respectively, given by (7) and (8). The system's achievable sum rate of the SBS is given by:

$$\mathbf{R}(\mathbf{q},\mathbf{a},\mathbf{p}) = \sum_{c=1}^{C}\left[\sum_{k=1}^{K} r_{k,c}^{\mathrm{FU}} + \sum_{u=1}^{U} r_{u,c}^{\mathrm{NU}}\right] \quad (9)$$

In order to fully realize the full potential of hybrid PD-SCMA, there is need to deploy resilient DNN based RA schemes for performance enhancement. At the receiver, joint MUD that iteratively decodes the received messages using log-MPA [2, 9], EPA [28, 29] in the code-domain and SIC in the power domain.

III. Optimization Problem Formulation

From (6) to (9), the RA problem results into a corresponding capacity optimization problem expressed as;

$$\begin{aligned}
\max_{\mathbf{q},\mathbf{a},\mathbf{p}} \quad & \mathbf{R}(\mathbf{q},\mathbf{a},\mathbf{p}) \\
\text{s.t.} \quad & \mathrm{C1}: \textstyle\sum_{c=1}^{C} r_{k,c}^{\mathrm{FU}} \geq R_{\min}^{k}, \forall k \\
& \mathrm{C2}: \textstyle\sum_{c=1}^{C} r_{u,c}^{\mathrm{FU}} \geq R_{\min}^{u}, \forall u \\
& \mathrm{C3}: \textstyle\sum_{k=1}^{K} q_{k,c}^{\mathrm{FU}} \leq d_f, \forall c \\
& \mathrm{C4}: \textstyle\sum_{u\in\mathcal{U}_c} A_{k,u}^{c} P_{u,c}^{\mathrm{NU}} \left|h_{u,c}^{\mathrm{NU}}\right|^2 \leq \mathcal{I}_{u\to k}^{c,\mathrm{th}}, \forall k \\
& \mathrm{C5}: q_{k,c}^{\mathrm{FU}} \in (0,1), \forall k, c \\
& \mathrm{C6}: P_{k,c}^{\mathrm{FU}} \geq 0, \forall k, c \\
& \mathrm{C7}: \textstyle\sum_{c=1}^{C} q_{k,c}^{\mathrm{FU}} P_{k,c}^{\mathrm{FU}} \leq P_{\max}^{\mathrm{FU}}, \forall k \\
& \mathrm{C8}: A_{k,u}^{c} P_{u,c}^{\mathrm{NU}} \left|h_{u,c}^{\mathrm{NU}}\right|^2 \geq q_{k,c}^{\mathrm{FU}} P_{k,c}^{\mathrm{FU}} \left|h_{k,c}^{\mathrm{FU}}\right|^2, \forall k, c, u \\
& \mathrm{C9}: \textstyle\sum_{u\in\mathcal{U}_c} A_{k,u}^{c} \leq D
\end{aligned} \quad (10)$$

In this problem, constraints C1 and C2 set the QoS rate requirement to ensure guaranteed performance of the *k*th FU and *u*th NU. Constraint C3 limits the number of users multiplexed on a single RE. Constraint C4 sets the tolerable pairing interference on each codebook on which a NU is co-multiplexed with a FU. Constraint C5 guarantees that a codebook is allocated to at most one FU. Constraints C6 and C7 ensure that the FU transmit power is non-negative and is within the maximum FU transmit power. The constraint C8 ensures SIC at the BS and lastly, C9 outlines the multiplexing bound *D*. However, solving (10) is complicated due to its mixed combinatorial nature. In addition, high coupling between optimization variables and combined computational cost encountered in CA, UP and PA exhaustive search for optimal EE is prohibitive. To address this problem, this work decomposes the optimization problem into three sub-problems namely; PA, CA and UC, considering the associated constraints and utilizes the proposed modified primal dual interior point method (mPD-IPM) to alternately solve the sub-problems.

IV. Proposed PD-SCMA Modified Primal Dual Interior Point Method Based Resource Allocation

The RA problem (10) is first decomposed into PA, CA and UC resource allocation sub-problems presented in the next sub-sections. This work proposes a modified primal dual interior point method (mPD-IPM) [32] to alternately generate near-optimal RA solutions for each sub-problem. These solutions are then considered as the labels for each stage of the DNN. The DNN is then used in the performance evaluation and enhancement of the proposed mPD-IPM algorithm. Unlike in [32], a smoothing approach similar to [33] is introduced to relax the PD-IPM parameters, guaranteeing both global and local convergence.

A. Stage 1: Power Allocation.

The starting stage of the resource allocation is the power allocation aimed at enhancing sum rate and the computing performance. The objective function of the PA sub-problem reduces to

$$\begin{aligned}
\mathbf{PA}: \max_{\mathbf{p}} \quad & \mathbf{R}(\mathbf{q},\mathbf{a},\mathbf{p}) \\
\text{s.t.} \quad & \mathrm{C1}: \textstyle\sum_{c=1}^{C} r_{k,c}^{\mathrm{FU}} \geq R_{\min}^{k}, \forall k \\
& \mathrm{C2}: \textstyle\sum_{c=1}^{C} r_{u,c}^{\mathrm{FU}} \geq R_{\min}^{u}, \forall u \\
& \mathrm{C3}: P_{k,c}^{\mathrm{FU}} \geq 0, \forall k, c \\
& \mathrm{C4}: \textstyle\sum_{c=1}^{C} q_{k,c}^{\mathrm{FU}} P_{k,c}^{\mathrm{FU}} \leq P_{\max}^{\mathrm{FU}}, \forall k \\
& \mathrm{C5}: A_{k,u}^{c} P_{u,c}^{\mathrm{NU}} \left|h_{u,c}^{\mathrm{NU}}\right|^2 \geq q_{k,c}^{\mathrm{FU}} P_{k,c}^{\mathrm{FU}} \left|h_{k,c}^{\mathrm{FU}}\right|^2 \\
& \forall k, c, u
\end{aligned} \quad (11)$$

where C1 to C5 are as described above.

The input data to the network is the output of the mPD-IPM which considers the channel gains $\left(h_{k,c}^{\mathrm{FU}} \text{ and } h_{u,c}^{\mathrm{NU}}\right)$ and the distance from the BS (s_k and s_u) for each FUs and NUs respectively as the metrics in its computation of the optimal PA, while the CA and UC is fixed. The mPD-IPM is characterized with iterating within feasible region and thus guarantees faster convergence rate to an optimal solution. The near-optimal power allocation of mPD-IPM algorithm is then given by $\mathbf{p} = \left\{P_{K,C}^{\mathrm{FU}}, P_{U,C}^{\mathrm{NU}}\right\}$.

$$P_{K,C}^{\mathrm{FU}} = \left[P_{k,c}^{\mathrm{FU}}\right]_{K\times C} \quad (12)$$

B. Stage 2: Codebook Assignment.

The codebook assignment (CA) forms the second stage of the RA to further improve the overall capacity. Based on the allocated powers in Stage IV-A, the corresponding codebook assignment to FUs sub-problem can be given as

$$\begin{aligned}
\mathbf{CA}: \max_{\mathbf{q}} \quad & \mathbf{R}(\mathbf{q},\mathbf{a},\mathbf{p}) \\
\text{s.t.} \quad & \mathrm{C1}: \textstyle\sum_{c=1}^{C} r_{k,c}^{\mathrm{FU}} \geq R_{\min}^{k}, \forall k \\
& \mathrm{C2}: \textstyle\sum_{k=1}^{K} q_{k,c}^{\mathrm{FU}} \leq d_f, \forall c \\
& \mathrm{C3}: q_{k,c}^{\mathrm{FU}} \in (0,1), \forall k, c
\end{aligned} \quad (13)$$

Similar to the PA sub-problem, the CA sub-problem utilizes the proposed mPD-IPM algorithm to generate the near-optimal codebook assignment matching to the FUs given by vector $\mathbf{q}$. The mPD-IPM utilizes the channel gains $\mathbf{h}$ and the allocated powers $\mathbf{p}$ to generate output $\mathbf{q}$.

$$\mathbf{q} = \left\{Q_{K,C}^{\mathrm{FU}}\right\} = \left[q_{k,c}^{\mathrm{FU}}\right]_{K\times C} \quad (14)$$

Algorithm 1 The Proposed mPD-IPM Resource Allocation Algorithm

1: **Initialization**: Initialize the sets: $\mathcal{U}, \mathcal{K}, \mathcal{C}$ and $\mathcal{L}$.

2: Initialize the set of NU and FU distances to the BS $\mathcal{S}$.

3: Initialize the set of NU and FU channel gains $\mathbf{H}$.

Stage 1: Power Allocation
Initialize equal powers to FUs set and equal powers to NUs set.
Initialize maximum tolerance ϵ, Maximum iterations $\boldsymbol{T}$ and iterations number τ.
while $|F_{\tau+1}(\mathbf{p}) - F_{\tau}(\mathbf{p})| > \epsilon$ or $\tau \leq \boldsymbol{T}$ **do**
  Solve (11) by PD-IPM
  Update $\mathbf{p} = \{P_{u,c}^{\mathrm{NU}}, P_{k,c}^{\mathrm{FU}}\}, \forall k, u$
  $\tau = \tau + 1$
end while
Output: p given by eqn (12).
Stage 2: Codebook Assignment
Initialize $P_{k,c}^{\mathrm{FU}}, \forall k$ obtained in **Stage 1**.
Initialize mother codebook $\mathbf{MC}^{K\times N}$.
for $c = 1, \cdots, C$ **do**
  for $k = 1, \cdots, K$ **do**
    while $\sum_{k=1}^{K} q_{k,c}^{\mathrm{FU}} \leq d_f$ **do**
      Solve (13) by PD-IPM
      Update $\mathbf{q} = \{Q_{K,C}^{\mathrm{FU}}\}, \forall k$
      $k = k + 1, c = c + 1.$
    end while
  end for
end for
Output: q given by eqn. (14).
Stage 3: User Clustering
Initialize $P_{k,c}^{\mathrm{FU}}, \forall k$ and $P_{u,c}^{\mathrm{NU}}, \forall c$ obtained in **Stage 1**.
Initialize the interference threshold $\mathcal{I}_{u\to k}^{c,\mathrm{th}}, \forall k, u$
Initialize the multiplexing bound D.
for $c = 1, \cdots, C$ **do**
  for $u = 1, \cdots, U$ **do**
    while $\sum_{u\in\mathcal{U}_c} A_{k,u}^{c} P_{u,c}^{\mathrm{NU}} |h_{u,c}^{\mathrm{NU}}|^2 \leq \mathcal{I}_{u\to k}^{c,\mathrm{th}}, \forall k$ **do**
      while $|A_{k,u}^{c} P_{u,c}^{\mathrm{NU}}| < D$ **do**
        Solve (15) by PD-IPM using the metric (16).
        Update $\mathbf{a} = [A_{k,u}^{c}]_{K\times U}$
        $k = k + 1, c = c + 1, u = u + 1.$
      end while
    end while
  end for
end for
Output: a given by eqn. (17).

C. Stage 3: User Clustering.

The last stage of the PD-SCMA RA is the user clustering (UC) which basically allows overloading by pairing NUs to the FUs assigned codebooks. This is achieved by clustering NUs with distinct powers for purposes of spectrum sharing, subject to an acceptable maximum interference threshold to guarantee SIC. Based on the allocated powers and the FUs codebook assignment from stage IV-A and IV-B respectively, the corresponding UC problem can now be given as;

$$\begin{aligned} \text{UC: } \max_{\mathbf{a}} \quad & \mathbf{R}(\mathbf{q}, \mathbf{a}, \mathbf{p}) \\ \text{s.t.} \quad & \text{C1: } \textstyle\sum_{c=1}^{C} r_{k,c}^{\mathrm{FU}} \geq R_{\min}^{k}, \forall k \\ & \text{C2: } \textstyle\sum_{u\in\mathcal{U}_c} A_{k,u}^{c} P_{u,c}^{\mathrm{NU}} |h_{u,c}^{\mathrm{NU}}|^2 \leq \mathcal{I}_{u\to k}^{c,\mathrm{th}}, \forall k \\ & \text{C3: } A_{k,u}^{c} P_{u,c}^{\mathrm{NU}} |h_{u,c}^{\mathrm{NU}}|^2 \geq q_{k,c}^{\mathrm{FU}} P_{k,c}^{\mathrm{FU}} |h_{k,c}^{\mathrm{FU}}|^2 \\ & \forall k, c, u \\ & \text{C4: } \textstyle\sum_{u\in\mathcal{U}_c} A_{k,u}^{c} \leq D \end{aligned} \tag{15}$$

In order to compute the optimal user clustering (UC), the UC input data-set to the mPD-IPM consisting of transmit powers, channel gains, interference threshold $\mathcal{I}_{u\to k}^{c,th}$ and the optimal cluster formation is generated by the mPD-IPM. The mPD -IPM UC is based on maximizing the channel quality metric difference denoted by $\chi_{m,k}^{c}$ [2] given by

$$\chi_{m,k}^{c} = \delta\big(\max(\theta_{K\times M}), \min(\mathbf{I}_{\min}^{c})\big) \tag{16}$$

The output of the mPD-IPM is then given as **a**:

$$\mathbf{a} = \left[A_{k,u}^{c}\right]_{K\times U} \tag{17}$$

The mPD-IPM exhibits the merit of guaranteeing faster ergodic convergence rates. The detailed complete mPD-IPM based RA is shown in Algorithm 1. The PD-IPM for nonlinear programming and its proof of convergence analysis is detailed in [34].

V. Proposed Deep Neural Network Based Resource Allocation

The proposed DNN-mPD-IPM resource allocation workflow strategy is a 3 -stage process; power allocation, codebook allocation and user clustering as illustrated in Fig. 2. The DNN network consists of one input layer, four hidden layers and one output layer as illustrated in Fig. 2 (a). The four hidden layers have 30012080 and 80 neurons, respectively [35]. The neuron receives information from the neuron of the previous layer. At each DNN-RA stage, the generated near optimal mPD-IPM RA solutions namely; power allocation **p**, codebook assignment **q** and user clustering a obtained respectively in (12), (14) and (17) are regarded as the DNN labels. The DNN model is then trained to approximate the label RA, and hence improved computing performance.

A. Stage 1: DNN - Power Allocation (DNN-PA).

At the DNN-PA stage, the DNN model is trained to approximate the mPD-IPM power allocation. The DNN-PA described in stage 1 of Fig. 2 (b) outlines the DNN structure development, data initialization, DNN model training, testing and sum-rate as the output. Denote by $\hat{\mathbf{p}}^{t}$ and $\hat{\mathbf{p}}^{t+1}$ respectively the set of output powers of the DNN at iteration t and t+1, respectively. The relation between $\hat{\mathbf{p}}^{t}$ and $\hat{\mathbf{p}}^{t+1}$ is given by the mapping equation (18):

$$\hat{\mathbf{p}}^{t+1} = \epsilon^{t}(\hat{\mathbf{p}}^{t}, \mathbf{p}) \tag{18}$$

where t and ϵ^{t} denotes the iteration number and the mapping. **p** denotes the label powers generated from the mPD-IPM (12).

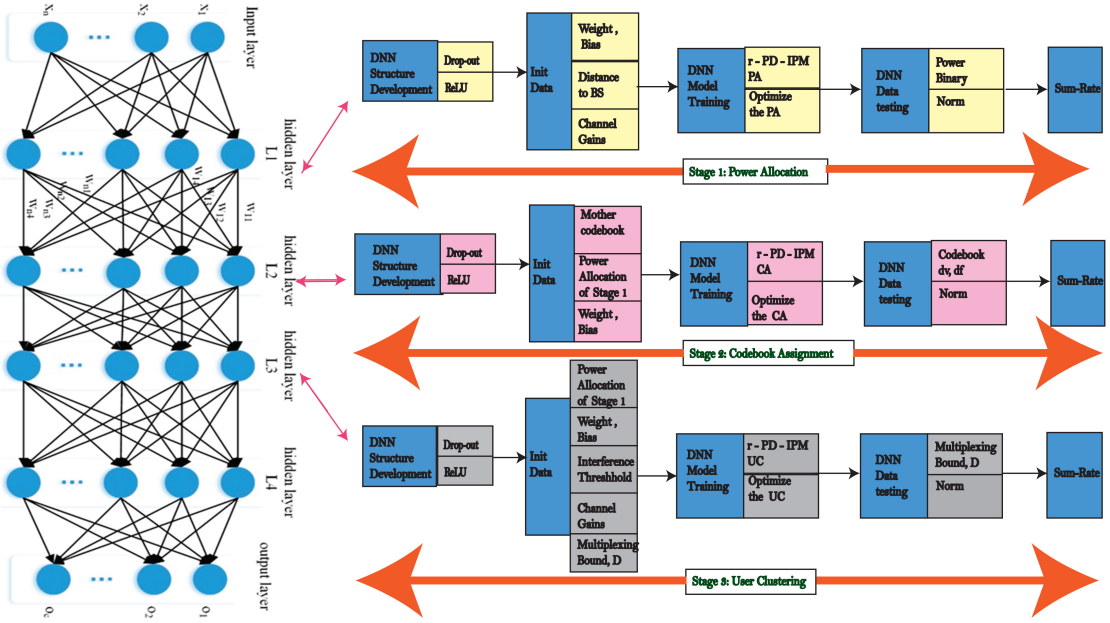

Fig. 2. DNN aided resource allocation mechanism.

The mapping from $\mathbf{p}$ and initialization $\hat{\mathbf{p}}^0$ to the final output $\hat{\mathbf{p}}^t$ given by the transmission expression (19):

$$\hat{\mathbf{p}}^t = f^t(f^{t-1}(\cdots f^1(f^0(\hat{\mathbf{p}}^0, \mathbf{p}), \mathbf{p})\cdots, \mathbf{p}), \mathbf{p}) \tag{19}$$

requires to be accurately approximated by an activation function and can be evaluated by

$$\max|\hat{\mathbf{p}}^t - \mathbf{p}|^2 \tag{20}$$

The output of the mPD-IPM is the optimized PAs with the total system sum-rate $\mathbf{R}_{\text{new}} - \mathbf{R}_{\text{old}} < 10^{-5}$ or a number of iterations >1000, as the termination condition. The DNN PA network model utilizes the MSE loss function given by

$$\min_{\hat{\mathbf{P}}} \parallel \hat{\mathbf{P}} - \arg\max_{\mathbf{P}} \mathbf{R}(\mathbf{Q}, \mathbf{A}, \mathbf{P}) \parallel. \tag{21}$$

In each hidden layer network, ReLU activation function described in (22) is applied since it saves and maps the features of the activated neurons besides mitigating gradient dispersion. The *i*th training samples are the tuples $\left(h_{k,c}^{\text{FU},t}, s_k, P_{k,c}^{\text{FU}}\right)$ and $\left(h_{u,c}^{\text{NU},t}, s_u, P_{u,c}^{\text{NU}}\right)$. The process is then executed many times to generate the validation set and the training set. The number of the validation set is smaller than the training set.

$$\text{ReLu}(x) = \begin{cases} x, & x \geq 0 \\ 0, & x < 0 \end{cases} \tag{22}$$

At the training stage, in order to optimize the DNN weights, the RMSprop algorithm [36] is used with decay rate set at 0.9. The batch size and the learning rate are determined using cross-validation. Optimization of the weights aims to minimize the loss function which is the MSE given in (21).

The testing stage involves testing the robustness of the trained network. The validation set of label powers obtained by mPD-IPM are passed to the DNN network to get the output. Then, the system capacity is calculated using the label powers and the output powers.

B. Stage 2: DNN - Codebook Assignment (DNN-CA).

Similar to the PA sub-problem, the CA sub-problem utilizes the generated mPD-IPM CA solution $\mathbf{q}$ obtained in (14) as the codebook assignment input labels to the DNN scheme. The DNN-CA illustrated in Stage 2 of Fig. 2 (b) is evaluated as follows; The relation between $\hat{\mathbf{q}}^t$ and $\hat{\mathbf{q}}^{t+1}$ is given by the mapping equation (23) while the transmission expression is given by (24).

$$\hat{\mathbf{q}}^{t+1} = \epsilon^t(\hat{\mathbf{q}}^t, \mathbf{q}) \tag{23}$$

$$\hat{\mathbf{q}}^t = f^t(f^{t-1}(\cdots f^1(f^0(\hat{\mathbf{q}}^0, \mathbf{q}), \mathbf{q})\cdots, \mathbf{q}), \mathbf{q}) \tag{24}$$

In this DNN-CA stage, we use ReLU activation function (22) in all but the last layer which uses a sigmoid activation function (25):

$$f_{\text{sig}}(x) = \frac{1}{1+e^{-x_p-1}} \tag{25}$$

At the training stage, since CA is a binary classification problem, the binary cross-entropy loss function is employed. The loss function Loss (W, b) is the binary cross-entropy of the DNN output $\hat{\mathbf{q}}$ and the mPD-IPM output $\mathbf{q}$ given as

$$\text{Loss}(W, b) = \frac{1}{KJ}\sum_i^{KJ} -(1-\mathbf{q}(i))\ln(1-\hat{\mathbf{q}}(i)) + \mathbf{q}(i)\ln\hat{\mathbf{q}}(i) \tag{26}$$

At the testing stage, the output of the DNN is converted to ones and zeros (with and without RE allocation) subject to C2 and C3 of the CA problem (13) to give output $\hat{\mathbf{q}}$.

Algorithm 2 DNN approaching mPD-IPM Resource allocation

1: **Initialization:** Initialize the DNN structure; i/o layers, no. of hidden layers, weights w and bias b.

2: **for** $m = 1$ to training epoch **do**
3: **for** $n = 1$ to num batch **do**
4: **DNN Model Training**
5: **Stage 1:** DNN training to approximate mPD-IPM power allocation by minimizing (21).
6: **Stage 2:** DNN training to approximate mPD-IPM codebook assignment by minimizing (26).
7: **Stage 3:** DNN training to approximate mPD-IPM user clustering by minimizing (30).
8: **end for**
9: **end for**
10: **DNN Data Testing:** Normalizing outputs for each sub problem; $\mathbf{p} = \left\{\left\{P_{k,c}^{\mathrm{FU}}\right\}_1^K, \left\{P_{u,c}^{\mathrm{NU}}\right\}_1^U\right\}$, $\mathbf{q} = \left\{q_{k,c}^{\mathrm{FU}}\right\}$, and $\mathbf{a} = \left\{A_{k,\mathrm{u}}^c\right\}$

C. Stage 3: DNN - User Clustering (DNN-UC).

The DNN-UC model computes the optimal user clustering (UC), through training the data-set of the transmit powers, FU codebook assignment and the optimal cluster formation generated by the mPD-IPM as shown in Stage 3 of Fig. 2 (b). The output a of the mPD-IPM obtained in (17) is considered as the UC labels/input to the DNN network. Similar to stages V-A and V-B, the DNN approximates the UC of the mPD-IPM within the acceptable multiplexing bounds in each codebook and gives the output $\hat{\mathbf{a}}$. The relation between $\hat{\mathbf{a}}^t$ and $\hat{\mathbf{a}}^{t+1}$ is given by the mapping (27) while the transmission expression is gives by (28):

$$\hat{\mathbf{a}}^{t+1} = \epsilon^t(\hat{\mathbf{a}}^t, \mathbf{a}) \tag{27}$$

$$\hat{\mathbf{a}}^t = f^t(f^{t-1}(\cdots f^1(f^0(\hat{\mathbf{a}}^0, \mathbf{a}), \mathbf{a})\cdots, \mathbf{a}), \mathbf{a}) \tag{28}$$

At the training stage, the learning process is formalized as a minimization of the cost function. To train the proposed DNN-UC, stochastic gradient descent is selected to update the weights and biases iteratively via back-propagation as follows;

$$\theta_{\tau+1} = \theta_\tau - \eta\nabla_\theta \mathbf{J}(\theta) \tag{29}$$

where $\theta_\tau, \tau, \eta, \nabla_\theta$ and $\mathbf{J}(\theta)$ respectively denote the parameter to be optimized, the iteration number, the scalar-valued step size, the derivative with respect to θ and the MSE cost function expressed as

$$\mathbf{J}(\theta) \Rightarrow \mathrm{MSE} = \frac{1}{D}\sum_{i=1}^{D} (\mathbf{a} - \hat{\mathbf{a}})^2 \tag{30}$$

Generally, Algorithm 2 outlines the DNN model training to approximate the mPD-IPM RA for the three sub-problems. Further, the overall alternate DNN aided RA (DNN-mPD-IPM) is presented in Algorithm 3.

Algorithm 3 The Alternate DNN aided mPD-IPM RA (DNN-mPD-IPM)

1: **Repeat:**
2: **Step 1: DNN - Power Allocation;** Update the NU and FU power allocation policy **P** with with random CA **Q**.
3: **Step 2: DNN - Codebook Assignment;** Update the FU codebook assignment policy **Q** with the PA **P** obtained in **Step 1**.
4: **Step 3: DNN - User Clustering;** Update the NU to FU user pairing in a codebook policy **A** with the PA **P** and CA **Q** obtained in **Step 1** and **Step 2**, respectively.
5: **Until** Convergence

VI. Convergence and Complexity Analysis

A. Convergence Analysis

The convergence of Algorithm 3 is influenced by both DNN data generation via mPD-IPM Algorithm 1 and the DNN training Algorithm 2. Algorithm 1 generates the labels using the mPD-IPM for the three sub-problems, PA, CA and UC. Similar to PD-IPM [34], mPD-IPM guarantees convergence of $O(1/k)$ in achieving the near-optimal solution for the PA, CA and UC sub-problems. After several PA, CA and UC operations in solving sub-problems (11), (13) and (15), respectively, the structure of the optimal resource allocation changes is presented as

$$F_0 \Rightarrow F_1 \Rightarrow F_2 \Rightarrow \cdots \Rightarrow F_l \Rightarrow \cdots \tag{31}$$

It is required that the sum-rate problem ensures a solution within the given constraints in (10). The overall system sum rate increases after each match operation l.

$$\Upsilon_{l-1}^l = \mathbf{R}_{\mathrm{total}}(F_l) - \mathbf{R}_{\mathrm{total}}(F_{l-1}) \tag{32}$$

The PA, CA and UC are bounded by maximum power, number of available codebooks and the multiplexing capacity bound, D respectively. In addition, the total sum rate has an upper bound in the hybrid PD-SCMA system since spectrum resources are limited and hence Algorithm 1 converges after optimal RA. Besides, we will show in Section VII that after a number of iterations, the MSE value flattens and the DNN-mPD-IPM Algorithm 3 converges to a fixed value.

B. Computational Complexity Analysis

Following the complexity analysis of PD-IPM [37], the complexity of mPD-IPM is outlined. It can be shown that for the small update method with accuracy parameter $\varepsilon > 0$, threshold parameter $\tau \geq 1$ and fixed barrier parameter θ usually set at $0 < \psi < 1$, the mPD-IPM algorithm requires $\mathcal{O}\left(\sqrt{n}\log\frac{n}{\varepsilon}\right)$. The output gives an ε approximate solution of convex quantization optimization. After derivations considering the PA, CA and UC sub-problem dimensions, the computational complexity of mPD-IPM can be given as,

$$\mathcal{O}\left(2K\log\frac{K^2}{\varepsilon} + U\log\frac{U^2}{\varepsilon} + \sqrt{UC}\log\frac{UC}{\varepsilon}\right) \tag{33}$$

The computational complexity of Algorithm 3 depends on both DNN data generation via mPD-IPM Algorithm 1 and the DNN training Algorithm 2. Generally, floating-point operations (FLOPs) are used to analyze the time complexity of a DNN [36]. For each fully connected layer of DNN without bias, the number of FLOPs is given by:

$$\mathrm{FLOPs} = (2I_1 - 1)O_l \tag{34}$$

where l, I_l and O_l respectively denote the index of the network layer, input dimension of the lth layer and output

dimension of the lth layer. For a fully connected DNN layer with bias, the number of FLOPs is given as

$$\text{FLOPs} = 2I_1O_l \tag{35}$$

Consequently, the number of FLOPs for all fully connected DNN layer in this model is given as

$$\begin{aligned}\text{FLOPs}&= 2\sum_{l=1}^{L+1} I_1O_l \\ &= 2(TNMh_1 + h_1h_2 + h_2h_3 + h_3h_4\end{aligned} \tag{36}$$

where L and T denote the number of network layers and the number of validation samples, respectively. The PA sub-problem input and output layers have dimensions of $K \times K$ and $U \times U$ for FUs and NUs respectively. The CA sub-problem has input and output layers with dimensions of $K \times C$ and lastly, the UC problem input and output layers dimensions is $U \times C$. The number of neurons in the four hidden layers are denoted by h_1, h_2, h_3 and h_4. Considering the input/output layer matrix dimensions of the CA, UC and PA sub-problems for FUs and NUs, the complexity comparison between DNN-mPD-IPM and mPD-IPM resource allocation can be given as follows;

$$\begin{aligned}&\mathcal{O}(4(T \cdot K \cdot K \cdot h_1 + h_1 \cdot h_2 + h_2 \cdot h_3 + h_3 \cdot h_4 \\ &+T \cdot K \cdot K \cdot h_4) \\ &+2(T \cdot U \cdot U \cdot h_1 + h_1 \cdot h_2 + h_2 \cdot h_3 + h_3 \cdot h_4 \\ &+T \cdot U \cdot U \cdot h_4) \\ &+ 2(T \cdot U \cdot C \cdot h_1 + h_1 \cdot h_2 + h_2 \cdot h_3 + h_3 \cdot h_4 \\ &+T \cdot U \cdot C \cdot h_4))\end{aligned} \tag{37}$$

From (37), the proposed DNN-mPD-IPM exhibits significant lower computation complexity than mPD-IPM RA model.

VII. Convergence and Complexity Analysis

A. Simulation Parameters Selection

The performance evaluation and comparison of the proposed mPD-IPM, proposed DNN-mPD-IPM and random resource allocation algorithms is investigated. In the random RA, the BS power is evenly distributed to the UEs, codebooks assigned to FUs and the NUs paired to FUs in a random manner. The detailed system parameters and assumptions for the uplink PDSCMA are presented in Table II [2, 9] while the DNN model simulation parameters for the uplink PD-SCMA system are presented in Table III.

In order to evaluate the loss function performance, the batch size 32, 64, 96 and 128 on the validation set is adopted.

Table II: Simulation Parameters

Parameters	Symbol	Values
Minimum FU QoS	$R_{\min}$	0.01bps/Hz
Error variance	σ_ε^2	0.01
RE Bandwidth	B_{ru}	$10MHz$
Number of FUs	K	$4-24$
Number of NUs per layer	U	$1-6$
Number of Codebooks	$C(N,d_v)$	$\frac{N!}{(N-d_v)!\,d_v!}$
Number of REs	N	$4-6$
Signal to Noise Ratio	SNR	$32dB$
Noise variance	$\sigma_{k,n}^2$	$-125dBm$
Distance between NUs and BS	d_{NU}	$20-40(m)$
Distance between FUs and BS	d_{FU}	$100-150(m)$
BS peak power	P	$43dBm$
Interference threshold	$\mathcal{I}_{k\to m}^c$	$10^{-5.5}$ W

Table III: DNN Model Simulation Parameters

Parameters	Values
Training data	140000
Validation data	40000
Hidden layers	4
Number of neurons in a layer	300/120/80/80
Activation functions	ReLU/Sigmoid
Loss functions	MSE/Binary Cross-Entropy
Batch size	64
Training / Validation Epoch	300
Learning rate	0.001
Decay rate	0.9

It is observed in Fig. 3 that the DNN converges within 300 iterations. The convergence rate reduces as the batch size enlarges. In this model, the smallest MSE for the validation set is arrived at a batch size of 64, hence its selected. Very small and very large batch sizes make the learning process noisier and fluctuating, essentially extending the time it takes the algorithm to converge [36]. Thus it can be observed that below 64, the MSE performance reduces due to noise. Furthermore, the learning rate affects the convergence on the training and validation set. Fig. 4 presents the system MSE system with respect to the number of iterations. A higher learning rate causes the NN to learn faster while a very small learning rate results to the NN falling into a local optimum. From Fig. 4, beyond 300 iterations, the MSE stabilizes and when the learning rate is 0.001, the MSE becomes the smallest. The performance drops beyond this rate. These parameters are hence adopted for this DNN model application.

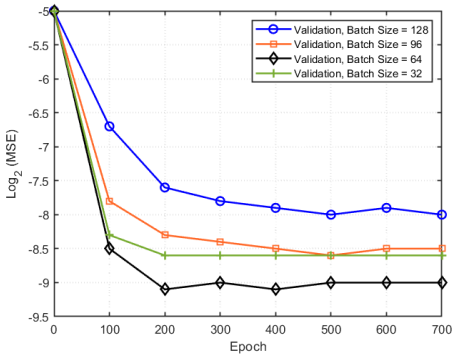

Fig. 3. MSE versus epoch for different validation batch sizes.

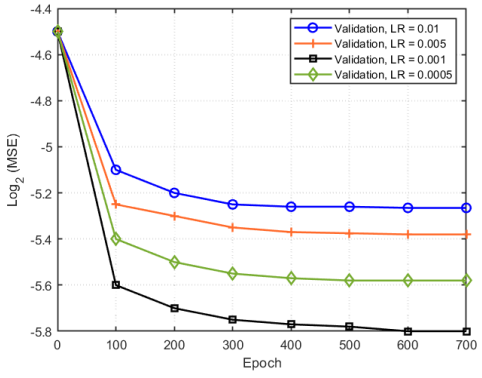

Fig. 4. MSE versus epoch for different learning rates.

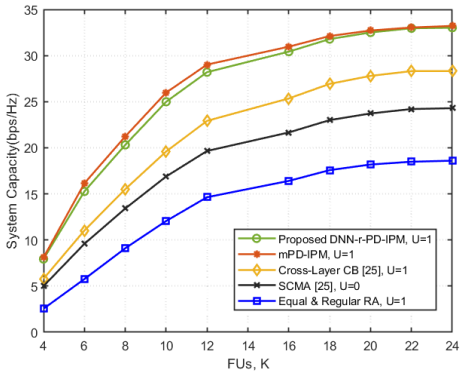

Fig. 5. The system capacity versus the number of FUs, *K*.

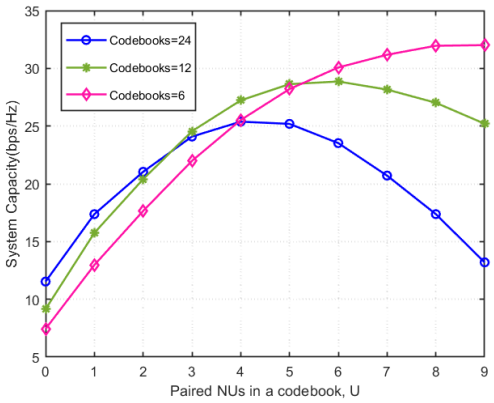

Fig. 6. The system capacity versus the number of NUs, U.

B. Capacity Performance

In Fig. 5, the system capacity versus the number of FUs for different algorithms is presented. In this performance analysis, the proposed DNN-mPD-IPM algorithm is evaluated and compared with the mPD-IPM, cross-layer codebook allocation [25] and random RA algorithms with U=1 multiplexed NUs in a codebook and, also compared with SCMA, which basically it is a PD-SCMA with U=0. In all the schemes, the system capacity increases with increasing number of FUs in the system. Besides, it is observed that the mPD-IPM algorithm achieves a higher system capacity compared to the rest of the schemes. The proposed combined DNN-mPD-IPM algorithm realizes a close approximation to the mPD-IPM, inevitably with less computational time. Besides, DNN-mPD-IPM RA algorithm enhances the efficiency gain of the hybrid PD-SCMA compared to the other considered schemes. The equal PA, random CA and UC scheme performs the least due to inefficient resource utilization associated.

The uplink PD-SCMA capacity performance for the proposed DNN-mPD-IPM vs the number of paired NUs U in a codebook is presented in Fig. 6 for diverse number of codebooks. As the number of NUs, U grows, the system capacity increases to a maximum value, beyond which, pairing additional NUs collapses the performance as a result of the aggravated interference in the codebook and complexity in SIC decoding. It is observed that using few codebooks, as shown with C=6, a larger number of NUs U can be paired with minimal performance deterioration unlike for higher number of codebooks, experiencing much more interference.

The impact of the FUs minimum QoS R_{min} on the system capacity at different number of codebooks is presented in Fig. 7. The performance analysis is done with the number of NUs clustered in a codebook, U=4. At C=6, the system capacity steadily decreases with increase in the minimum QoS requirements of FUs R_{min}. As number of codebooks used C increases (C=12; C=24), the system capacity steeply nosedives with increase in R_{min}. Additional FUs with inadequate channel conditions in the system require enhanced power and codebook resources in order to satisfactorily meet the minimum QoS requirements.

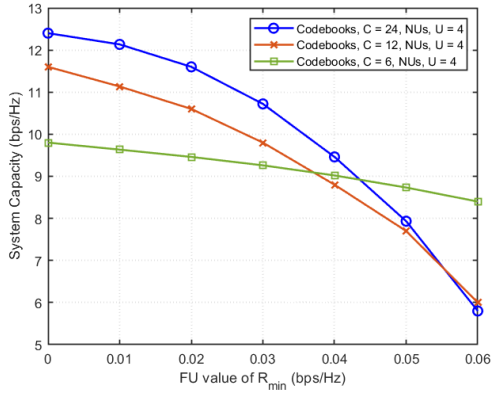

Fig. 7. The system capacity versus R_{min} for the FUs with U=4 for different number of codebooks.

C. Computing Performance

Fig. 8 presents a comparison of the execution times for different PD-SCMA resource allocation schemes with a fixed number of NUs per codebook and fixed number of codebooks at U=2 and C=6 respectively. It is observed that mPD-IPM algorithm has a higher execution time due to the increased resource exchanges iterations before convergence. The cross-layer codebook allocation scheme proposed in [25] with U=2 encounters twice the execution time of SCMA with U=0. The proposed DNN-mPD-IPM that learns to approximate the proposed mPD-IPM has an execution time that is approximately 70% lower than mPD-IPM.

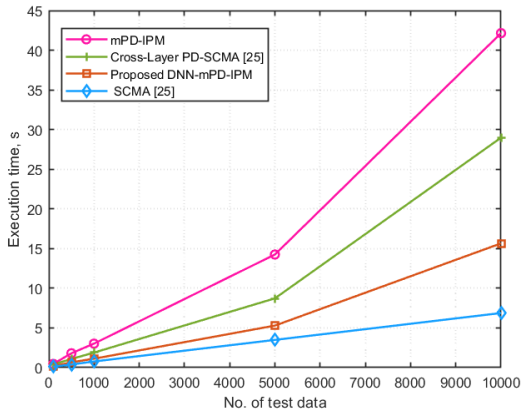

Fig. 8. Execution time for different RA schemes.

Fig. 9 shows a comparison of the execution times in a DNN-mPD-IPM aided PD-SCMA resource allocation

with varied number of the clustered NUs, U and the number of codebooks fixed at C=6. It is observed that as the number of clustered NUs increases, the execution time grows exponentially. Since a PD-SCMA with $U = 0$ is equivalent to a SCMA, then the execution time is lower as the element of user clustering is eliminated. Besides, additive codebooks, user clustering and the resulting interference computations drastically increases the execution time.

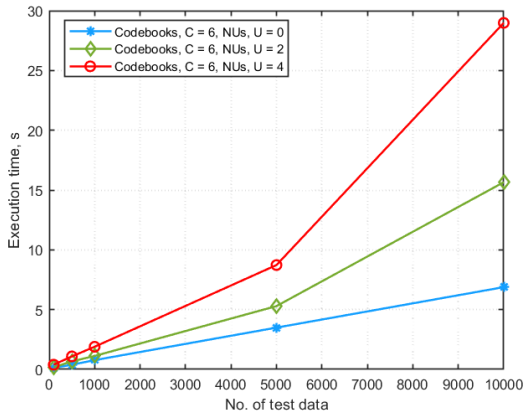

Fig. 9. Execution time for the RA in the uplink PD-SCMA with different number of paired NUs, U.

VIII. Conclusion

The formulated MINLP capacity optimization problem for uplink PD-SCMA system is decomposed into CA, UC and PA sub-problems. This work proposes two resource allocation schemes namely, mPD-IPM and DNN-mPD-IPM to enhance system capacity, computational efficiency and convergence performance. Hybrid NOMA systems, which combine multiple access schemes, introduce additional complexity in resource allocation. The interaction between different access schemes can complicate the deep learning model's ability to make accurate predictions and require significant computational resources and time for training. Additionally, Hybrid NOMA systems often operate in highly dynamic environments with rapidly changing conditions, which can make it difficult for deep learning models to adapt in real-time. The proposed schemes generally improve the system performance hence can be adopted in overloaded systems as compared to generic resource allocation schemes. However, further work is recommended in exploring an optimal multi-user detection scheme for such an overloaded system in order to fully realize the benefits of the hybrid NOMA. Moreover, further exploratory research on the application of the deep learning models for dynamically changing channel environments and diversified devices needs is required. Besides, other ML algorithms such as LSTM and CNN should be considered for RA in hybrid NOMA for performance evaluation purposes.

Conflict of Interest

The authors declare no conflict of interest.

Author Contributions

Simon Chege conducted the research, wrote the paper and analyzed the data; Tom Walingo analyzed the results and reviewed the work; all authors had approved the final version.

Acknowledgment

The authors would like to thank Centre for Radio Access and Rural Technologies (CRART) at University of Kwa Zulu Natal (UKZN) for supporting this work.

References

[1] Z. Ding, X. Lei, G. K. Karagiannidis, R. Schober, J. Yuan, and V. K. Bhargava, "A survey on non-orthogonal multiple access for 5g networks: Research challenges and future trends," *IEEE Journal on Selected Areas in Communications*, vol. 35, no. 10, pp. 2181–2195, 2017.

[2] S. Chege and T. Walingo, "Energy efficient resource allocation for uplink hybrid power domain sparse code non-orthogonal multiple access heterogeneous networks with statistical channel estimation," *Trans. on Emerging Telecommunications Technologies*, vol. 32, no. 1, e4185, 2021.

[3] N. I. Kim and D.-H. Cho, "Hybrid multiple access system based on non-orthogonality and sparse code," in *Proc. 2017 IEEE Wireless Communications and Networking Conference*, 2017. doi: 10.1109/WCNC.2017.7925930

[4] M. Moltafet, N. Mokari, M. R. Javan, H. Saeedi, and H. Pishro-Nik, "A new multiple access technique for 5G: Power domain sparse code multiple access (PSMA)," *IEEE Access*, vol. 6, pp. 747–759, 2018.

[5] S. Sharma, K. Deka, V. Bhatia, and A. Gupta, "Joint power-domain and scma-based noma system for downlink in 5 g and beyond," *IEEE Communications Letters*, vol. 23, no. 6, pp. 971–974, 2019.

[6] T. Sefako and T. Walingo, "Biological resource allocation algorithms for heterogeneous uplink PD-SCMA NOMA networks," *IEEE Access*, vol. 8, pp. 194950–194963, 2020.

[7] M. Rebhi, K. Hassan, K. Raoof, and P. Charg é, "Sparse code multiple access: Potentials and challenges," *IEEE Open Journal of the Commu nications Society*, vol. 2, pp. 1205–1238, May 2021.

[8] S. M. R. Islam, N. Avazov, O. A. Dobre, and K.-S. Kwak, "Powerdomain Non-Orthogonal Multiple Access (NOMA) in 5 G systems: Potentials and challenges," *IEEE Communications Surveys & Tutorials*, vol. 19, no. 2, pp. 721–742, 2017.

[9] S. Chege and T. Walingo, "Multiplexing capacity of hybrid PD-SCMA heterogeneous networks," *IEEE Trans. on Vehicular Technology*, vol. 71, no. 6, pp. 6424–6438, 2022.

[10] S. A. H. Mohsan, Y. Li, A. V. Shvetsov, J. Varela-Ald ás, S. M. Mostafa and A. Elfikky, "A survey of deep learning based NOMA: State of the art, key aspects, open challenges and future trends," *Sensors*, vol. 23, no. 6, 2023.

[11] V. Andiappan and V. Ponnusamy, "Deep learning enhanced NOMA system: A survey on future scope and challenges," *Wireless Personal Communications*, vol. 123, pp. 839–877, Sep., 2022.

[12] G. Gui, H. Huang, Y. Song, and H. Sari, "Deep learning for an effective non-orthogonal multiple access scheme," *IEEE Trans. on Vehicular Technology*, vol. 67, no. 9, pp. 8440–8450, 2018.

[13] W. Saetan and S. Thipchaksurat, "Application of deep learning to energy-efficient power allocation scheme for 5G SC-NOMA system with imperfect SIC," in *Proc. 2019 16th Int. Conf. on Electrical Engineering/Electronics, Computer, Tele-communications and Information Technology*, 2019, pp. 661–664.

[14] N. Ye, X. Li, H. Yu, A. Wang, W. Liu, and X. Hou, "Deep learning aided grant-free NOMA toward reliable low-latency access in tactile internet of things," *IEEE Trans. on Industrial Informatics*, vol. 15, no. 5, pp. 2995–3005, 2019.

[15] Y. Azimi, S. Yousefi, H. Kalbkhani, and T. Kunz, "Energy-efficient deep reinforcement learning assisted resource allocation for 5G -RAN slicing," *IEEE Trans. on Vehicular Technology*, vol. 71, no. 1, pp. 856–871, 2022.

[16] D. Huang, Y. Gao, Y. Li, M. Hou, W. Tang, S. Cheng, X. Li, and Y. Sun, "Deep learning based cooperative resource allocation in 5

g wireless networks," *Mobile Networks and Applications*, pp. 1–8, 2018.
[17] K. I. Ahmed, H. Tabassum, and E. Hossain, "Deep learning for radio resource allocation in multi-cell networks,' *IEEE Network*, vol. 33, no. 6, pp. 188–195, 2019.
[18] P. Yu, F. Zhou, X. Zhang, X. Qiu, M. Kadoch, and M. Cheriet, "Deep learning-based resource allocation for 5 g broadband tv service," *IEEE Trans. on Broadcasting*, vol. 66, no. 4, pp. 800–813, 2020.
[19] R. Dong, C. She, W. Hardjawana, Y. Li, and B. Vucetic, "Deep learning for radio resource allocation with diverse quality-of-service requirements in 5g," *IEEE Trans. on Wireless Communications*, vol. 20, no. 4, pp. 2309–2324, 2021.
[20] M. Kim, N.-I. Kim, W. Lee, and D.-H. Cho, "Deep learning-aided scma," *IEEE Communications Letters*, vol. 22, no. 4, pp. 720–723, 2018.
[21] P. Liu, J. Lei, and W. Liu, "A deep reinforcement learning scheme for scma-based edge computing in IoT networks," in *Proc. GLOBECOM 2022 2022 IEEE Global Communications Conf.*, 2022, pp. 5044–5049.
[22] P. Yang, W. Wang, W. Mao, G. Zhang, J. Cai, D. Hong, H. Zhu, J. Zhang, and S. Chen, "A deep learning based automatic interference avoidance resource allocation scheme for scma systems," *Journal of Physics. Conference Series*, vol. 2095, no. 1, 012052, 2021.
[23] J. Lin, S. Feng, Y. Zhang, Z. Yang, and Y. Zhang, "A novel deep neural network based approach for sparse code multiple access," *Neurocomputing*, vol. 382, pp. 52–63, 2020.
[24] S. Sharma and Y. Hong, "A hybrid multiple access scheme via deep learning-based detection," *IEEE Systems Journal*, vol. 15, no. 1, pp. 981–984, 2021.
[25] S.-M. Tseng and W.-Y. Chen, "Cross-layer codebook allocation for uplink scma and pdnoma-scma video transmission systems and a deep learning-based approach," *IEEE Systems Journal*, vol. 17, no. 1, pp 294–305, 2023.
[26] C. Lin, Q. Chang, and X. Li, "A deep learning approach for mimo-noma downlink signal detection," *Sensors*, vol. 19, no. 11, p. 2526, 2019.
[27] L. Dai, B. Wang, Z. Ding, Z. Wang, S. Chen, and L. Hanzo, "A survey of non-orthogonal multiple access for 5g," *IEEE Communications Surveys & Tutorials*, vol. 20, no. 3, pp. 2294–2323, 2018.
[28] S. Chege and T. Walingo, "Mimo hybrid pd-scma noma uplink transceiver system," *IEEE Access*, vol. 10, pp. 88 138–88 151, 2022.
[29] S. Chege, T. Walingo, and F. Derraz, "Codebook design for pd-scma noma systems," *IEEE Access*, vol. 11, pp. 13421–13431, 2023.
[30] X. Fu, D. Le Ruyet, B. Fontana Da Silva, and B. F. Uchôa-Filho, "A simplified sphere decoding-based detector for generalized scma codebooks," *IEEE Access*, vol. 10, pp. 516–534, 2022.
[31] L. Xiang, Y. Liu, C. Xu, R. G. Maunder, L.-L. Yang, and L. Hanzo, "Iterative receiver design for polar-coded scma systems," *IEEE Trans. on Communications*, vol. 69, no. 7, pp. 4235–4246, 2021.
[32] Y. Zhu, D. Liu, and Q. Tran-Dinh, "A new primal-dual algorithm for a class of nonlinear compositional convex optimization problems," *arXiv preprint arXiv*:2006.09263, 2020.
[33] X.-W. Liu, Y.-H. Dai, and Y.-K. Huang, "A primal-dual interior-point relaxation method with global and rapidly local convergence for nonlinear programs," *Mathematical Methods of Operations Research*, vol. 96, no. 3, pp. 351–382, 2022.
[34] I. Griva, D. F. Shanno, and R. J. Vanderbei, "Convergence analysis of a primal-dual interior-point method for nonlinear programming," *Optimization Online (http://www. Optimization online. org/DB HTML/2004/07/913. html)*, 2004.
[35] O. A. Montesinos López, A. Montesinos López, and J. Crossa, "Fundamentals of artificial neural networks and deep learning," *Multivariate Statistical Machine Learning Methods for Genomic Prediction*, Springer, 2022, pp. 379–425.
[36] N. Yang, H. Zhang, K. Long, H.-Y. Hsieh, and J. Liu, "Deep neural network for resource management in noma networks," *IEEE Trans. on Vehicular Technology*, vol. 69, no. 1, pp. 876–886, 2019.
[37] X. Cai, G. Wang, and Z. Zhang, "Complexity analysis and numerical implementation of primal-dual interior-point methods for convex quadratic optimization based on a finite barrier," *Numerical Algorithms*, vol. 62, no. 2, pp. 289–306, 2013.

Simon Chege received the B.Sc. degree in electrical and communications engineering from Moi University, Kenya, the M.Sc. degree in electrical and electronic engineering from JNTU-Anantapur, India, and the PhD in electronic engineering from the University of KwaZulu-Natal, Durban, South Africa. He is working with Moi University, Kenya as a lecturer in the Department of Electrical and Communication Engineering. He is also currently undertaking a post-doctoral research fellowship at the University of Kwa Zulu Natal. He has published and reviewed papers in peer reviewed journals. He is also a TPC member at WIDECOM and IEEE AFRICON conferences. Currently, his research interests include wireless communications, multi-radio access technologies, wireless sensor networks, machine learning and smart cities.

Tom Walingo received the B.Sc. degree in electrical and communications engineering from Moi University, Kenya, the M.Sc. degree in electronic engineering from the University of Natal, and the Ph.D. degree in electronic engineering from the University of KwaZulu-Natal, Durban, South Africa. He is currently a researcher with the Center of Radio Access and Rural Technology and a professor in communications and computer engineering at the University of KwaZulu-Natal. He has authored many peer-reviewed journals and conference papers. His current research interests include digital and wireless communications, satellite communications, and wireless sensor networks. He was a recipient of several research awards, including the SAIEE ARJ 2013 Award. He is an editor/reviewer for several journals in his field.